

# Comparative study of optical kinetics in single and dual poly3-methylthiophene-based solid electrochromic devices

Ulises León-Silva · M. E. Nicho · Hailin Hu

Received: 14 February 2007 / Revised: 30 March 2007 / Accepted: 3 May 2007 / Published online: 7 June 2007  
© Springer-Verlag 2007

**Abstract** An electrochemically deposited poly3-methylthiophene (P3MT) thin film has been used as the primary electrochromic element in a solid two-electrode electrochromic device (ECD) with a viscous polymeric electrolyte (PE) of polymethyl methacrylate and lithium perchlorate co-dissolved in ethylene and propylene carbonates. The counter-electrode of the ECD was a transparent conductive (indium-tin oxide, ITO) glass (single ECD) or a polyaniline (PANI)-coated ITO glass (dual ECD). Dual P3MT-PANI-based ECDs exhibit a lower optical switch potential (less than 0.5 V) and a faster color change speed (around 1 s) compared with the single devices, independent on the lithium salt concentration and the viscosity of the polymeric electrolyte. Electrochemical impedance spectra of both types of ECDs were analyzed at zero bias. It indicates that the use of the secondary electroactive element leads to a lower counterion diffusion resistance as well as to a larger counter-ion storage capacity in the electrochromic element/polymeric electrolyte interfaces. Consequently, the oxidation–reduction potential is lower, and the charge transfer process is faster in the dual devices than those in the single ones.

**Keywords** Solid electrochromic devices · Poly3-methylthiophene · Optical kinetics · Electrochemical impedance spectra · Polymeric electrolyte

## Introduction

Electrochromism means the color change of a working electrode in an electrochemical cell when it is under an oxidation–reduction process. A solid electrochromic device (ECD) is formed by sticking the working and counter electrodes together with a polymeric or viscous electrolyte in-between. In a single solid ECD, only the working electrode is electrochromic (primary), whereas in a dual one, the counter electrode is also electrochromic (secondary) and must be optically complementary with the primary one to result in the coloring-bleaching of the device during the redox process.

The electrochromic properties of conducting polymers were discovered in the decade of the 1980s. Thin films of polyaniline (PANI) and poly3-methylthiophene (P3MT) have been used separately as the primary electrochromic elements and a conducting glass substrate as the counter-electrode with a polymeric or gel electrolyte [1–4]. It is observed that both the switch potential and speed in PANI-based ECDs are influenced by the type of polymeric electrolyte (PE) used for ion conduction and storage. A polyethylenimine (PEI)–H<sub>2</sub>SO<sub>4</sub> based aqueous acidic electrolyte permits a relatively low switch potential ( $\pm 1.2$  V) and a rapid color change [5, 6], whereas a non-aqueous polymethyl methacrylate (PMMA)–LiClO<sub>4</sub>–acetonitrile (ACN) gel originates a higher switch potential (from  $\pm 1.5$  to  $\pm 2$  V) in a PANI-based single ECD with a slow electrochromic kinetics [5]. A P3MT-based ECD works

U. León-Silva · M. E. Nicho  
Centro de Investigación en Ingeniería y Ciencias Aplicadas,  
Universidad Autónoma del Estado de Morelos,  
Av. Universidad 1001, Col. Chamilpa,  
Cuernavaca 62210 Morelos, Mexico

H. Hu (✉)  
Departamento de Materiales Solares, Centro de Investigación en  
Energía, Universidad Nacional Autónoma de México,  
Priv. Xochicalco S/N,  
Temixco 62580 Morelos, Mexico  
e-mail: hzh@cie.unam.mx

only with non-aqueous electrolytes; with the same PMMA–LiClO<sub>4</sub>-ACN gel, the oxidation potential of the single P3MT devices was relatively high ( $\geq 1.5$  V) with a slow optical switch speed [7]. In the wavelength region from 400 to 600 nm approximately, PANI and P3MT are optically complementary: PANI bleaches as reduced and P3MT does when it is oxidized, and vice versa [5, 7].

On the other hand, during the redox process of the single PANI-based ECDs with PMMA–LiClO<sub>4</sub> as the electrolyte, the capacitive current reaches into its maximum in less than 60 ms, although the corresponding optical transitory curve could take more than 1 min to reach its equilibrium value [5]. It means that the electron injection/extraction into/from the ITO material is much faster than charge transfer processes occurring at the ITO/PANI and PANI/electrolyte interfaces. The main reason for slow electrochromic kinetics in conducting polymer-based single ECDs should be related to an asymmetric electrochemical reaction during the oxidation–reduction process of the devices. Indium–tin oxide (ITO) coated glass substrates are mostly used as the counter-electrodes in ECDs; they have shown good stability to repeated cyclic voltammeteries (CV) in a three-electrode cell with liquid electrolyte of LiClO<sub>4</sub>-propylene carbonate and are colorless in both the reduced and neutral forms [8]. The introduction of a secondary electrochromic element has been reported in conducting polymer-based ECDs with both polymeric [9, 10] and liquid electrolytes [11]. It is observed that the dual devices show rapid electrochromic kinetics and require small potential (less or equal to 1 V) for the color change. However, a direct comparison of the optical switch speed between the single and dual ECDs has not been reported. In this work, the optical kinetics of single and dual P3MT-based ECDs will be shown as a function of the electrolyte salt concentration as well as the viscosity of the polymeric electrolyte. Electrochemical impedance spectra (EIS) of these devices are studied under zero polarization for the comparative purpose to visualize the effect of the secondary electroactive element on the optical kinetics of the dual ECDs.

## Experimental

### Materials

P3MT thin films were electrochemically deposited on ITO-coated glass substrates (8–12  $\Omega$  per square, Delta Technologies, USA). These were previously cleaned with neutral soap, distilled water, and acetone and dried with air. A three-electrode system potentiostat of BAS 100 B/W was used with Ag/AgCl as reference electrode and Pt wire as counter one. The bath composition was: 0.1 M 3-methylthiophene (MT, Aldrich, 98%) and 0.1 M LiClO<sub>4</sub> (Aldrich,

95%) in ACN. Electrochromic P3MT films were formed on ITO glass at 2.5 V (vs Ag/AgCl) for 5 s, resulting in a film thickness of about 230 nm. PANI thin films were grown on ITO glass substrates by chemical bath deposition as reported otherwise [12]. Briefly, distilled aniline monomer was added in a 0.1 M NH<sub>4</sub>S<sub>2</sub>O<sub>8</sub> and 2 M HCl aqueous solution at 3–5°C under stirring, and then clean ITO substrates were introduced into the freshly prepared solution. Green PANI thin films of about 120 nm thick were obtained on ITO glass after 1 h of deposition. The thickness of the conducting polymer films was measured by using a Veeco Dektar profilometer with probe diameter of 12.5 mm and probe load of 2 mg.

Polymeric electrolyte was prepared by dissolving PMMA (Aldrich,  $M_w=120,000$ ) and LiClO<sub>4</sub> in a mixture of propylene and ethylene carbonates. Table 1 shows the composition of four types of PMMA–LiClO<sub>4</sub> electrolytes used in this work: PE3, PE5, PE5b, and PE7. As the molecular weight of PMMA monomer unit is 100.09 g/mol, close to that of the lithium salt (106.34 g/mol), propylene carbonate (102.09 g/mol), and ethylene carbonate (88.06 g/mol), the weight percent is similar to the molar ratio between different components of these electrolytes.

### Device and characterization

Solid ECDs were prepared by combining different electrodes with each polymeric electrolyte. They can be classified in four groups:

- ITO/PE/ITO
- ITO/P3MT/PE/ITO (single P3MT ECD)
- ITO/ PE/ PANI/ITO (single PANI ECD) and
- ITO/P3MT/PE/PANI/ITO (dual ECD).

The average thickness of the electrolytes was about 260  $\mu\text{m}$ , and the devices were sealed with epoxy giving an effective area of about 1 cm<sup>2</sup>.

**Table 1** Composition of PMMA/LiClO<sub>4</sub>-based polymer electrolytes (PE)

Name of PE	PE3	PE5	PE5b	PE7
Weight ratio of LiClO <sub>4</sub> / PE	3:100	5:100	5:100	7:100
Weight ratio of PMMA/ solvents	0.385:1	0.357:1	0.538:1	0.329:1
Percentage (wt%)				
PMMA	27	25	35	23
Propylene carbonate	35	35	30	35
Ethylene carbonate	35	35	30	35
LiClO <sub>4</sub>	3	5	5	7
Total	100	100	100	100

Optical transmittance spectra of the devices were recorded on a Shimadzu Spectrophotometer UV-VIS 1601. The applied voltage pulses on ECDs were generated by a homemade electrical control unit. The kinetic or transitory transmittance curves of the ECDs were measured at a selective wavelength, in this case, at 550 nm. The reason for which the green color was chosen is that the peak of the sun radiation is in the green portion of the visible spectrum, and the human eyes have adapted to the nature of the sunlight reaching them and function best in green light [13]. EIS of the devices were carried on a Solatron SI 1260 impedance/gain-phase analyzer coupled with a SI 1287 electrochemical interface. The EIS measurements were made in the frequency range from 1 MHz to 0.05 Hz, and the amplitude of the alternate signals was 50 mV. All the devices were under zero polarization at room temperature during the EIS tests.

## Results and discussion

### Electrochromic responses of ECDs

Figure 1 shows optical transmittance spectra of a P3MT and a PANI-based single ECDs under applied potentials of  $-1.4$  V and  $+1.4$  V with positive polarization on P3MT- or PANI-coated ITO side and negative one on the counter electrode (ITO glass). The polymeric electrolyte was PE5 in both devices, which contained a lithium salt concentration of 5 wt%. It is observed that P3MT is colored at a reduction ( $-1.4$  V) and bleached at an oxidation ( $+1.4$  V) process in the most part of visible region (400–600 nm), and vice versa in 600–1,100 nm wavelength range. The electrochromic kinetics of the same P3MT single ECD in Fig. 1 is slow under voltage applications

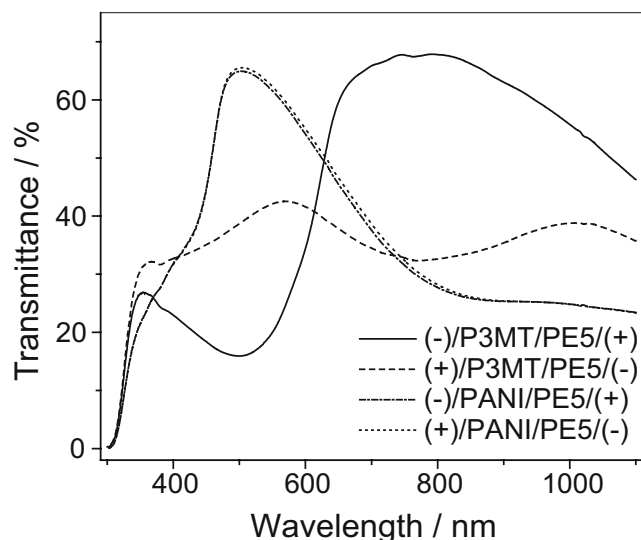


**Fig. 1** Optical transmittance spectra of single ITO/P3MT/PE5/ITO and ITO/PE5/PANI/ITO ECDs at  $-1.4$  and  $+1.4$  V polarization

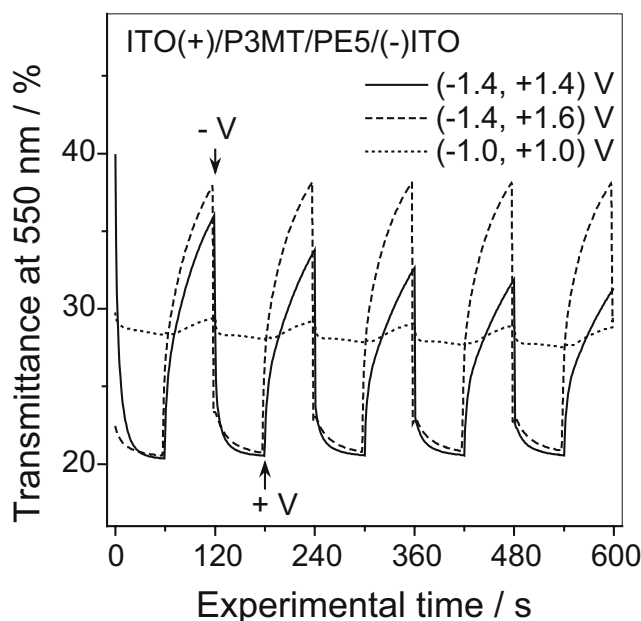


**Fig. 2** Transitory transmittance at 550 nm of single ITO/P3MT/PE5/ITO ECD under potential applications of  $\pm 1.0$  V,  $\pm 1.4$  V and  $-1.4$ ,  $+1.6$  V. Positive bias on P3MT

of  $\pm 1.0$ ,  $\pm 1.4$ , and  $-1.4$  to  $+1.6$  V (Fig. 2). At  $\pm 1.0$  V, the optical contrast, which is the maximum transmittance difference between the bleached and colored states, is around 2%, quite low for application purpose. By increasing the applied potentials, the optical contrast of the devices increased, but the optical switching speed is still slow. Notice that the apparent instable kinetics at  $\pm 1.0$  V and  $\pm 1.4$  V should be related to the slow oxidation process in the device because the higher oxidation potential ( $+1.6$  V) was applied after the  $\pm 1.4$  V test and the corresponding kinetic curve is more stable than the lower one. Similar phenomenon is also observed in Fig. 3 for the same type of the devices but with different lithium salt concentration in PE: 3 wt% (PE3) and 7 wt% (PE7). Together with Fig. 2, it is observed that the devices with a lower concentration of  $\text{LiClO}_4$  in the electrolytes (PE3 and PE5) show a lower bleaching (oxidation) speed than that of the coloring (reduction) one, but in the case of a higher concentration of lithium salt (PE7), the contrary occurred.

To understand the effect of lithium salt concentration in the polymeric electrolytes on the electrochromic kinetics of the single P3MT-based ECDs, optical transmittance spectra of these devices and the P3MT film on ITO glass under zero potential bias were shown in Fig. 4. The P3MT film (solid line) originates two broad absorption peaks: one of polaron band around 1.6 eV and the other of HOMO–LUMO transitions at about 2.5 eV. It is observed that the relative intensity of the polaron band in the P3MT ECDs increases as the  $\text{LiClO}_4$  salt concentration increases in the polymeric electrolyte, which is quite logic by considering that P3MT film can be doped (oxidized) by the lithium salt

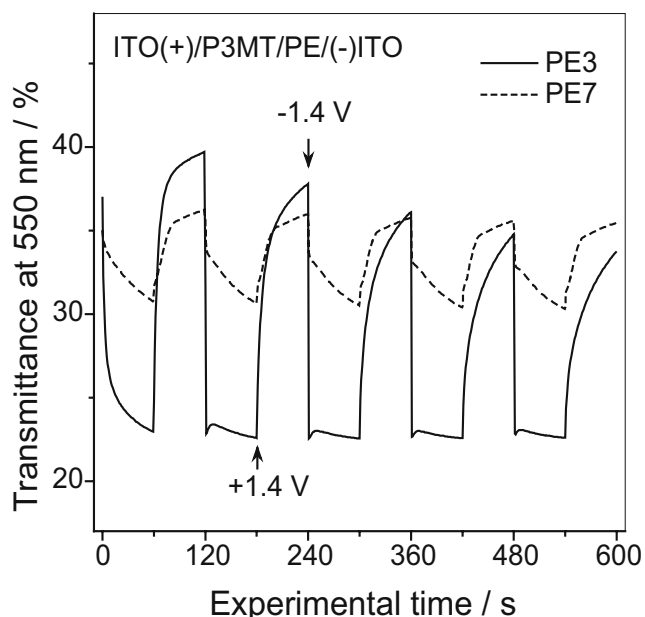


**Fig. 3** Transitory transmittance at 550 nm of single ITO/P3MT/PE3/ITO and ITO/P3MT/PE7/ITO under potential applications of  $\pm 1.4$  V. Positive bias on P3MT

insertion. The higher the  $\text{LiClO}_4$  concentration in the electrolyte, the higher the percentage of the lithium salt that should be diffused into the P3MT polymer, and more oxidized will be the conducting polymer. Consequently, for single P3MT ECDs under the same external potential bias, a highly oxidized P3MT in the P3MT/PE7 device should be easier to be oxidized (faster oxidation) and more difficult to be reduced (slower reduction), whereas a lower oxidized P3MT in the P3MT/PE3 or P3MT/PE5 device should give a slower oxidation speed and a higher reduction one.

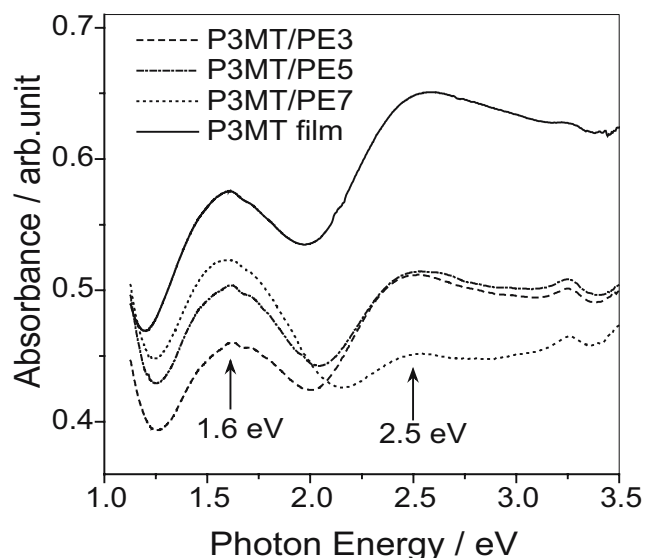


**Fig. 4** Optical absorption spectra of P3MT film as well as P3MT-based single ECDs with PE3, PE5, or PE7 as the polymeric electrolyte at 0 V

When the ITO glass was replaced by the PANI-coated ITO glass, the optical kinetics of the dual devices shows a drastic change. As the color change in PANI electrode is small or negligible for polarization less than or equal to  $\pm 1.4$  V, the color change in a dual P3MT ECD with PANI as the complementary electroactive element should be predominated by P3MT. Figure 5 shows the optical transmittance spectra of an ITO/P3MT/PE5/PANI/ITO device under  $-1.4$  and  $+1.4$  V applied voltages with positive polarization on P3MT film. Compared with the P3MT single ECD of Fig. 1, the presence of PANI film in the dual device increases the optical contrast in 400–600 nm region and reduces a little the transmittance in near-infrared region (700–1,100 nm) during the reduction process in P3MT. Figure 6 shows the transmittance values at 550 nm of the same dual ECD of Fig. 5 as a function of time for different potential pulses:  $\pm 0.5$ ,  $\pm 1.0$ , and  $\pm 1.4$  V. An applied potential of  $\pm 1.0$  V on the dual device can cause a 20% of transmittance change in comparison with a 2% in the P3MT single one under the same polarization (Fig. 2). At the same time, the optical switch speed in the dual devices is also significantly improved: The switching time is reduced from minutes to seconds compared with the P3MT single ECDs.

To estimate the optical switch speed in an ECD, the fitting of the bleaching curves can be done with:

$$T_b = T_{b0}[1 - \exp(-t/\tau)] \quad (1)$$

and the coloring ones with:

$$T_c = T_{c0} \exp(-t/\tau) \quad (2)$$

Here,  $T_b$  and  $T_c$  are optical transmittance values at certain wavelength in bleaching and coloring process,

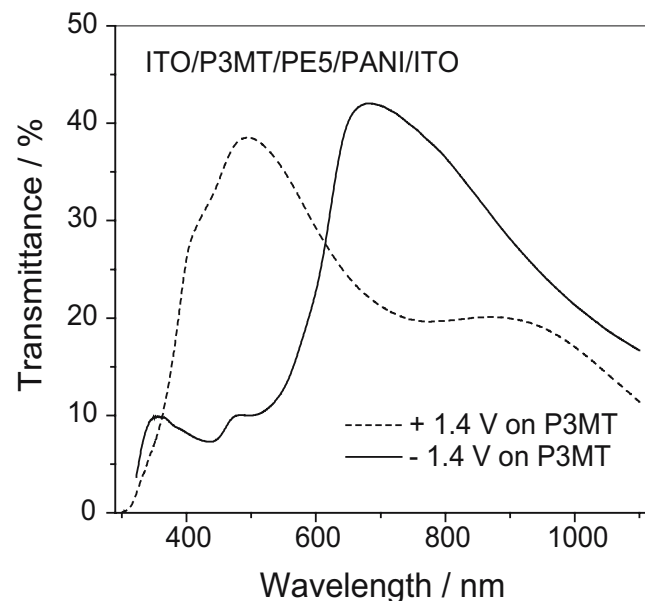


**Fig. 5** Optical transmittance spectra of dual ITO/P3MT/PE5/PANI/ITO device under  $-1.4$  and  $+1.4$  V polarizations

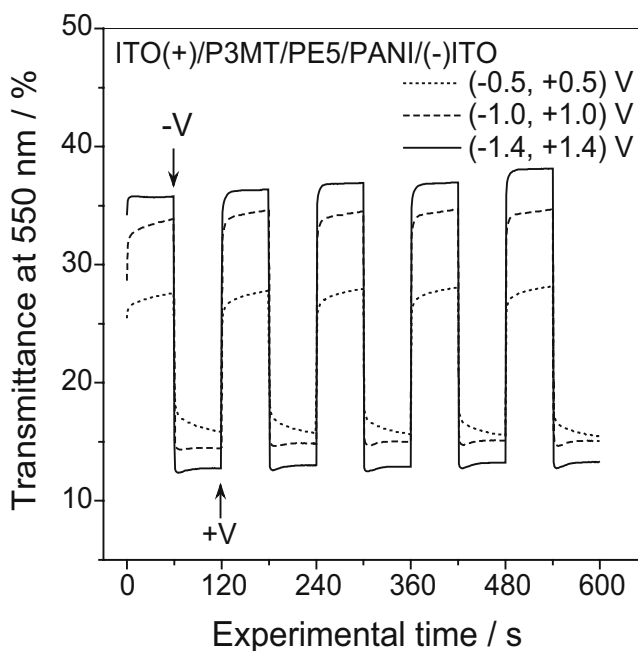


**Fig. 6** Transitory transmittance at 550 nm of dual ITO/P3MT/PE5/PANI/ITO ECDs under potential applications of  $\pm 0.5$ ,  $\pm 1.0$ , and  $\pm 1.4$  V. Positive bias on P3MT

respectively,  $T_0$  is the initial transmittance value in each process, and  $\tau$  (unit, s) is the interval of time that the device takes to reach the 63% of the equilibrium value in each kinetic curve. The  $\tau$  is the parameter that describes the optical switch speed in an ECD; the smaller the  $\tau$  value, the faster the color changes. In the dual ITO/P3MT/PE5/PANI/ITO device, Eqs. 1 and 2 fit quite well the color change processes. For example, the bleaching curves at  $-1.4$  V in Fig. 6 can be fitted by

$$T_b = 67.89[1 - \exp(-t/0.94)] \quad (3)$$

and the coloring ones at  $+1.4$  V in Fig. 6 by

$$T_c = 197.88 \exp(t/0.47). \quad (4)$$

It means that the dual ECD takes about 1.5 s for bleaching and about 0.75 s for coloring.

For the single ITO/P3MT/PE5/ITO device, however, it is found that the best fitting for bleaching process was using two right terms of Eq. 1: for  $-1.4$  V bleaching curves in Fig. 2,

$$T_b = 7.07[1 - \exp(-t/2.65)] + 15.97[1 - \exp(-t/50.39)] \quad (5)$$

and for the coloring ones at  $+1.4$  V in the same figure:

$$T_c = 30.03 \exp(-t/1.01) + 4.79 \exp(-t/9.52). \quad (6)$$

The use of two terms for the kinetic curve fitting has been reported previously for single PANI ECDs [5]. It suggests that the optical kinetics in single conducting

polymer-based ECDs can be visualized as a rapid charge transfer at the ITO/conducting polymer interface (the term with the smaller  $\tau$ ) and a slow ion exchange at the conducting polymer/electrolyte one (the term with the larger  $\tau$ ). Among these two  $\tau$ 's, the larger one determines the time lapse on which the device needs to reach the equilibrium value of the optical transitory curve. Therefore, the bleaching time was about 80 s and the coloring one about 15 s for the mentioned single P3MT ECD, substantially larger than those of the corresponding dual device.

As the lithium salt concentration in polymer electrolytes is changed to less (PE3) or more (PE7), the same electrochromic behavior is observed in PE3- and PE7-based dual ECDs (Fig. 7). Similarly, with the same 5 wt% of  $\text{LiClO}_4$  but more PMMA and less solvent content, the PE5b-based dual ECD also gives a rapid color change and reasonably optical contrast (Fig. 7). It seems that the large optical contrast and the rapid optical switch are the intrinsic properties of the dual ECDs, independent on the lithium salt concentration and the viscosity of the electrolytes.

#### Electrochemical impedance spectra of ECDs at zero bias

#### ECDs with less viscous electrolytes (PE3, PE5 and PE7)

The electrochromic kinetics of the conducting polymer-based ECDs can be better understood by analyzing their EIS results. Figure 8a exhibits the Nyquist plot [14] of the sandwiched ITO/PE5/ITO device. The characteristic semi-circle at low frequencies suggests a non-blocking PE5/ITO interface, the same behavior observed for the ITO electrode

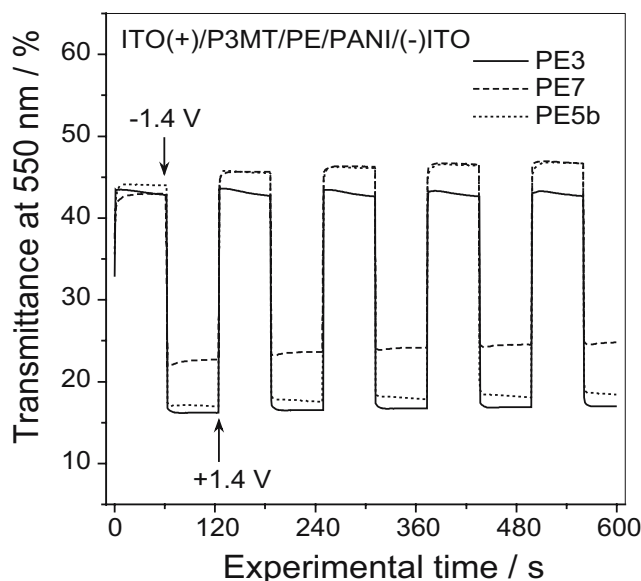


**Fig. 7** Transitory transmittance at 550 nm of ITO/P3MT/PE3/PANI/ITO, ITO/P3MT/PE7/PANI/ITO and ITO/P3MT/PE5b/PANI/ITO under potential applications of  $\pm 1.4$  V. Positive bias on P3MT

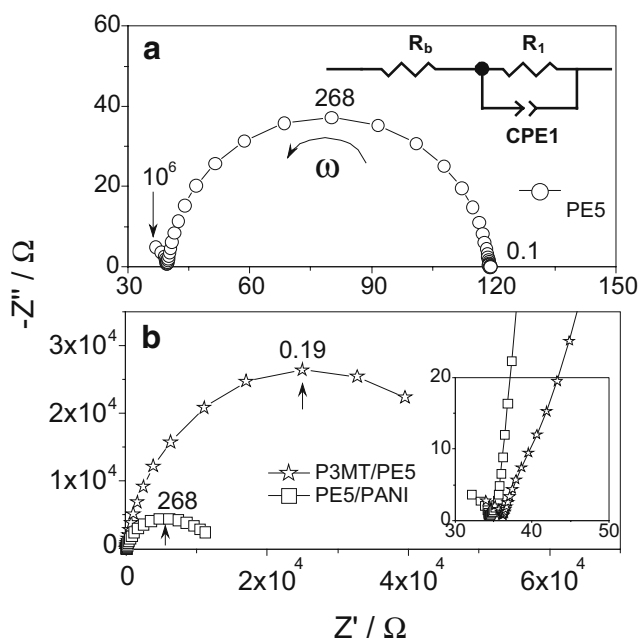


**Fig. 8** Nyquist plots of **a** ITO/PE5/ITO (open circle), **b** ITO/P3MT/PE5/ITO (open star), and ITO/PE5/PANI/ITO (open square). Insets **a** The equivalent circuit for the three devices, **b** the same plots in the high frequency region. The numbers in the figure are frequency values in Hz

in liquid electrolytes [8]. Similar Nyquist plots were also observed for PE3 and PE7 sandwiched devices with slightly different parameter values (not showed here). It suggests that the low viscosity of these three polymeric electrolytes permits easy lithium ion diffusion and the posterior accumulation of the ions on the ITO surface to participate the charge transfer and electrode reaction. Ignoring the geometric capacitance of the electrolyte, the equivalent circuit for the Nyquist plot in Fig. 8a consists in two parts (inset of the same figure): a high frequency resistor  $R_b$  and a low frequency RC of an electrode reaction resistance  $R_1$  in parallel with a non-ideal electrode capacitor, the constant phase element 1 (CPE1) [14].  $R_b$  should only be related to the ionic conduction in the bulk electrolyte and

was about  $40 \Omega$  for PE5 (Table 2), giving a bulk conductivity of the electrolyte of about  $6.5 \times 10^{-4} \Omega^{-1} \text{cm}^{-1}$ . The RC part of the circuit describes the charge transfer and diffusion process in the PE/ITO interface. The rate of the electrode reaction is reflected in the value of  $R_1$ , the larger the  $R_1$  the slower the reaction rate [15], and the capacitive element evidences the charge accumulation capacity in the ITO electrode. The value of CPE1 shows a low charge accumulation capacity ( $1 \times 10^{-5} \Omega \text{s}^{-0.95}$ ) at the double layers of the PE5/ITO interface for the ITO/PE5/ITO device.

For P3MT and PANI single ECDs with PE5 as the polymeric electrolyte, their Nyquist plots are similar (Fig. 8b), a high frequency  $R_b$  with a semicircle at low frequency region. Compared with the ITO/PE5/ITO device (Fig. 8a), the presence of an electrochromic element on one of the two ITO electrodes increases the charge accumulation capacitance CPE1, but it still remains in the same order of magnitude, about  $10^{-5} \Omega \text{s}^{-0.92}$  (Table 2). However, the charge transfer resistance  $R_1$  increases more than three orders of magnitude due to the introduction of the electroactive polymer: about  $60 \text{ k}\Omega$  and  $11 \Omega$  for the P3MT/PE5 and PE5/PANI devices, respectively (Table 2). The large values of  $R_1$  indicate that the accumulated charges at the polymer/electrolyte interfaces could not be easily inserted into or extracted from the polymeric films. This charge transfer impediment should come from the low charge accumulation capacity at the counter-electrode interface, the ITO/electrolyte one, incapable of storage sufficient amount of the counter-ions for the electrochemical reaction at the working electrode.

When a secondary electrochromic element is introduced in a solid ECD, Gazotti et al. [9] reported that the Nyquist plot of the device contains two semicircles at middle and low frequency regions. Each semicircle is represented with a resistor  $R$  in parallel with a CPE. The higher frequency semicircle corresponds to the charge transfer ( $R_2$ , CPE2) and the lower one to the ion diffusion at the conducting polymer/electrolyte interfaces ( $R_1$ , CPE1). In the present

**Table 2** Fitting parameters for EIS spectra at zero bias of PE5- and PE5b-based devices

Device: ITO/...../ITO	High frequency zone				Low frequency zone		
	$R_b$ ( $\Omega$ )	$R_2$ ( $\Omega$ )	CPE2 ( $\Omega \text{s}^{-n_2}$ )	$n_2$	$R_1$ ( $\Omega$ )	CPE1 ( $\Omega \text{s}^{-n_1}$ )	$n_1$
PE5							
PE5	40	–	–	–	79	$1.0 \times 10^{-5}$	0.95
P3MT/PE5	38	–	–	–	60609	$1.9 \times 10^{-5}$	0.92
PE5/PANI	35	–	–	–	11052	$2.7 \times 10^{-5}$	0.91
P3MT/PE5/PANI	40	12	$3.5 \times 10^{-5}$	0.80	319	$1.2 \times 10^{-3}$	0.84
PE5b							
PE5b	53	–	–	–	–	$7 \times 10^{-6}$	0.96
PE5b/PANI	51	–	–	–	–	$1.4 \times 10^{-5}$	0.96
P3MT/PE5b	53	–	–	–	–	$1.8 \times 10^{-5}$	0.91
P3MT/PE5b/PANI	44	6	$6.6 \times 10^{-5}$	0.80	–	$2.7 \times 10^{-3}$	0.92

work, a similar behavior is observed in the ITO/P3MT/PE5/PANI/ITO device at zero polarization (Fig. 9). For the small semicircle at high frequency region (268 Hz to 100 kHz), the curve fitting gives the values of  $R_2=12.1 \Omega$  and  $CPE2=3.5 \times 10^{-5} \Omega s^{-0.80}$ . For the larger one at low frequency region (0.1 to 268 Hz),  $R_1=319 \Omega$  and  $CPE1=1.2 \times 10^{-3} \Omega s^{-0.84}$ . The Bode plots [14] of the four PE5 based devices (Fig. 10) exhibit a better visualization about the charge transfer and diffusion processes in these devices at different frequency ranges. Single P3MT and PANI ECDs give a broad maximum and almost  $80^\circ$  phase angle at low frequency region ( $10^{-2}$  to  $10^2$  Hz) with high resistance (absolute values of  $Z$ , which is defined as  $Z=Z'-Z''$ ), whereas the dual P3MT/PE5/PANI device separates charge transfer and ion diffusion process into two well-defined frequency regions: an almost in-phase charge transfer at high frequency region and a  $\sim 40^\circ$  phase angle for ion diffusion process at low frequency region. For PE3- and PE7-based devices, similar EIS were obtained compared with those of PE5 ones (not showed here).

*ECDs with a more viscous electrolyte (PE5b)*

With a more viscous electrolyte PE5b, the ITO/PE5b/ITO device shows a blocking Nyquist plot (Fig. 11), different than the less viscous PE5 one (Fig. 8). It means that the rate of charge transfer is much faster than the diffusion of the lithium ions at the PE5b/ITO interface (diffusion control). The equivalent circuit for this device is a bulk resistor  $R_b$  in series with an interfacial non-ideal capacitor, the CPE1 (inset of Fig. 11).  $R_b$  is  $53 \Omega$  in this case, higher than that of

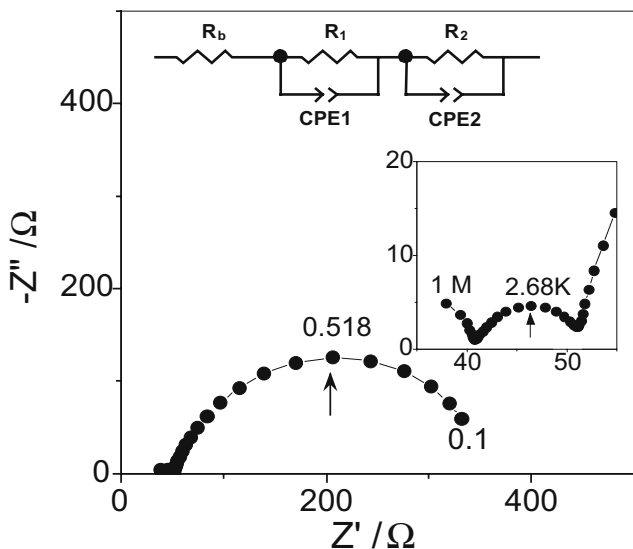


**Fig. 9** Nyquist plot of dual ITO/P3MT/PE5/PANI/ITO ECD. *Inset* The equivalent circuit of the device and the same plot in the high frequency region. The *numbers* in the figure are frequency values in Hz

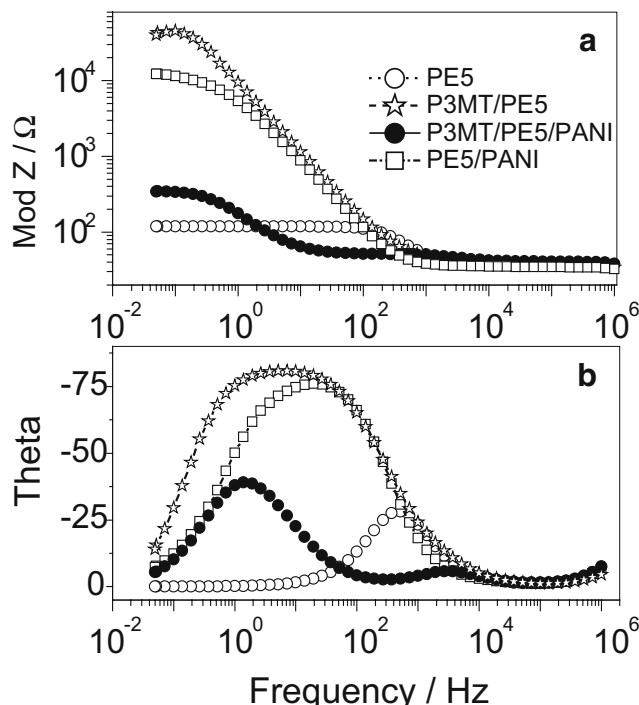


**Fig. 10** Bode plots of ITO/PE5/ITO, ITO/P3MT/PE5/ITO, ITO/PE5/PANI/ITO and ITO/P3MT/PE5/PANI/ITO devices

PE5, which is reasonable for the presence of a major percentage of PMMA and less amount of the solvents. The value of CPE1 is about  $7 \times 10^{-6} \Omega s^{-0.96}$ , a little smaller than that of the ITO/PE5/ITO device (Table 2). The Nyquist plot of the PANI single ECD with PE5b as electrolyte exhibits the same characteristic like that of the PE5b only device (Fig. 11). Consequently, it can also be described by the same equivalent circuit for the ITO/PE5b/ITO device with a bulk resistance  $R_b$  of about  $51 \Omega$  and a diffusive line almost perpendicular to the  $Z'$  axis described by a CPE1 with the value of  $1.4 \times 10^{-5} \Omega s^{-0.96}$  (Table 2). On the other hand, P3MT-based single ECD with PE5b as the electrolyte shows two segments in its diffusive line (Fig. 11): a line almost parallel to  $Z''$  axis at low frequency region (0.1 to 518 Hz) and the second one at high frequency region (1 to 100 kHz) that forms an angle close to  $45^\circ$  with the horizontal axis. The first one could be well fitted by the same equivalent circuit shown in inset of Fig. 11 (Table 2). The second line could come from a blocking and rough P3MT/PE5b interface or from a non-blocking one that is smooth and exhibiting a Warburg impedance [14] due to the slow diffusion of the reactant species ( $Li^+$  ions) to the interface [16]. As our electrochemically deposited P3MT thin films show a rougher surface than that of the chemical bath deposited PANI films [17], the contact of the P3MT film with a very viscous polymeric electrolyte (PE5b) could lead to a non-uniform atomic contact between them and results in a rough interface. Similar impedance spectra were also reported for the P3MT electrodes in liquid electrolytes

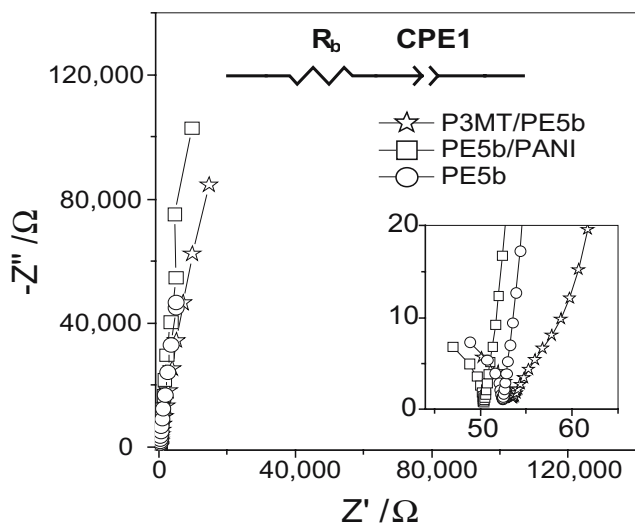


**Fig. 11** Nyquist plots of ITO/PE5b/ITO (*open circle*), ITO/PE5b/PANI/ITO (*open square*) and ITO/P3MT/PE5b/ITO (*open star*). *Insets* The same plot in the high frequency region and the equivalent circuit for the three devices

and described by considering the P3MT electrode as a one dimensional cylindrical pore structure [18], with much higher values for the capacitance elements compared with that of the single P3MT/PE5b device.

The dual PE5b-based ECD, however, shows a small depressed capacitive semicircle in the middle–high frequency region (from 193 Hz to 51.8 kHz with the maximum  $Z''$  at 2.68 kHz, inset of Fig. 12), which relates to the charge transfer process at the interfaces formed by the conducting polymer-coated electrodes and the polymeric electrolyte. The charge transfer resistance is even smaller in this case ( $R_1=6\ \Omega$ , Table 2) than that of the dual ECD with PE5 as the electrolyte ( $R_1=12\ \Omega$ , Table 2). At low frequency region, a very much reduced diffusive line is shown in this case (Fig. 12), and the double layer element CPE2 is about 100-fold ( $2.7 \times 10^{-3}\ \Omega\ s^{-0.92}$ ) compared with those of the single P3MT ECD. The equivalent circuit for the dual ECD could be a bulk resistance ( $R_b$ ) in series with the charge transfer unit ( $R_2$  in parallel with CPE2) plus a second, CPE1 related to the double layer capacitor at electrolyte/conducting polymer interfaces (see inset in Fig. 12). The Bode plots of the PE5b-based devices are exhibited in Fig. 13, showing the dramatically diminish in the diffusive resistance at low frequency region in comparison with the single ECDs. It is worth to mention that the Nyquist and Bode plots of the PE5b-based dual device are both analytical and numerically similar to those for P3MT electrodes in the asymmetrical configuration (Pt|polymer|electrolyte) with liquid electrolytes at zero or oxidative polarization [19].

The main difference in the EIS of PE5- and PE5b-based dual ECDs is on the diffusive low frequency region: The former shows a resistor–capacitor (semicircle) and the latter a pure capacitor (line) behavior. It suggests that a less

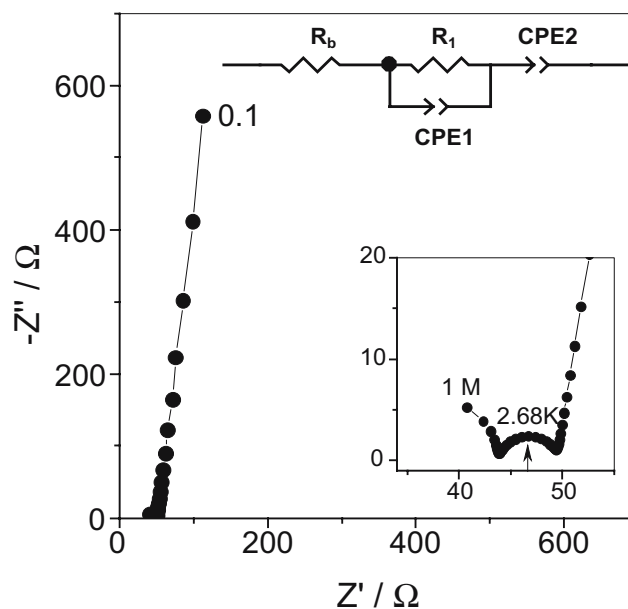


**Fig. 12** Nyquist plot of dual ITO/P3MT/PE5b/PANI/ITO ECD. *Insets* The same plot in the high frequency region and equivalent circuit for the device. The numbers in the figure are frequency values in Hz

viscous polymeric electrolyte such as PE5 (as well as PE3 and PE7) gives a slower charge accumulation process in comparison with the ion diffusion inside the electrochromic-conducting polymer films, which is reasonable if we consider that all the three less viscous electrolytes (PE3, PE5, and PE7) contain a significant amount of solvents and part of them should migrate into the electrochromic films

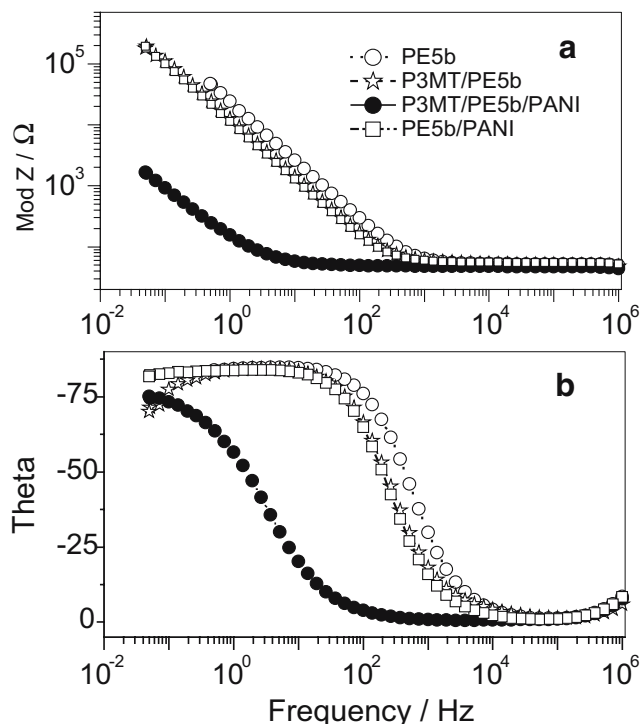


**Fig. 13** Bode plots of ITO/PE5b/ITO, ITO/P3MT/PE5b/ITO, ITO/PE5b/PANI/ITO and ITO/P3MT/PE5b/PANI/ITO devices



together with the lithium salt. This facilitates the diffusion of the ions inside the polymer film but at the same time causes a rapid association between the ions of opposite charge and consequently a slower charge accumulation in the electroactive polymer. The viscous PE5b electrolyte, however, contains fewer amounts of solvents, and their migration into the electroactive-conducting polymers is also less. Consequently, in this case, the diffusion speed of the ions is slower than the charge accumulation one inside the solid polymeric films.

#### Optical switch potential and color change speed in dual ECDs

The introduction of the secondary electroactive element in the single ECDs originates two notable changes in their EIS at zero bias: (1) the appearance of the small charge transfer semicircle at high frequency region and (2) the increase of the capacitance (and diminish of the resistance) in the diffusive semicircle (or line) at low frequency one. As the charge transfer semicircle increases with the polarization potential [9], the first fact indicates that the redox reaction initiates at lower potential in dual ECDs than in the single ones, which coincides with the electrochromic switch potential for these two types of ECDs. In the case of the diffusive semicircle (or line), the capacitance of the two-electrode device could be assimilated as the effective of two capacitances in series. Suppose that  $C_1$  is the capacitance of one electrode/electrolyte interface and  $C_2$ , the other. The effective capacitance,  $C_E$ , of two electrode/electrolyte interfaces in series is equal to:

$$\frac{1}{C_E} = \frac{1}{C_1} + \frac{1}{C_2} \quad (7)$$

As the value of  $C_E$  should be always close to the minimum of  $C_1$  and  $C_2$ , the low diffusive capacitance of single ECDs should be associated to the ITO/polymeric electrolyte interfaces ( $\sim 10^{-5} \Omega \text{ s}^{-0.92}$ ), and the high capacitance value of dual devices should reflect the real charge accumulation capacity of the conducting polymers in contact with the electrolytes ( $\sim 10^{-3} \Omega \text{ s}^{-0.84}$ ).

The effect of the PANI presence on the optical switch potential of the P3MT dual ECDs can be envisaged by considering the same electrochromic polymer in a three-electrode cell with the liquid electrolyte  $\text{LiClO}_4\text{-ACN}$ , whose volume can be considered as infinite for the P3MT-coated working electrode. The large liquid volume permits the storage of the  $\text{Li}^+$  ions during the oxidation process of the P3MT electrode so that the polymer can change the color from dark brown (reduced) to transparent blue (oxidized) in a potential range from +0.0 to +0.4 V (vs Ag/AgCl), respectively [7]. In the case of the P3MT solid ECDs, the thickness of the polymeric electrolyte represents

a much more reduced volume compared with the liquid one for both the working and counter electrodes. During the oxidation process, positively charged P3MT needs the  $\text{ClO}_4^-$  ion incorporation to achieve the phase transition from reduced to oxidized one. As ITO/electrolyte interface shows a low capacitance to storage the  $\text{Li}^+$  counter ions, these cannot be separated far away from perchlorate ions by the space limitation. An electrical potential should be created inside the electrolyte to impede the insertion of  $\text{ClO}_4^-$  ions into the P3MT-coated working electrode. On the other hand, the space-charge effect should be observed in a 230-nm thick P3MT film [20], which could be partially responsible for that potential. A larger applied potential can help to reduce the impeding potential, but the optical kinetics is still limited. As the ITO counter-electrode is replaced by a PANI/ITO one, this shows an almost 100-fold diffusive capacitance, which permits a larger charge accumulation on the counter-electrode interface, necessary for the redox processes occurring in both electrodes of the devices and consequently a much larger amount of  $\text{ClO}_4^-$  ions are available to be inserted into P3MT, leading to the color change at a lower potential ( $\pm 0.5$  V or lower, Fig. 6) as if it were immersed in an infinite liquid electrolyte. Finally, the faster optical switch speed in the P3MT dual ECDs is due to the replacement of slow lithium ion accumulation kinetics in the ITO/electrolyte interface by a rapid one in the PANI/electrolyte interface.

#### Conclusions

Electrochromic behavior of solid P3MT-based ECDs has been studied by using the ITO glass (single) or PANI-coated ITO glass (dual) as counter-electrode. For a single P3MT ECD, an external voltage not less than 1.4 V is required to induce a notable color change in the devices with a bleaching time of about 80 s and the coloring of about 15 s. Whereas for a dual P3MT-PANI one, less than 1 V is sufficient to obtain the same color change and the optical switch time is reduced to about 1.5 s for bleaching and about 0.75 s for coloring, independent on the lithium salt concentration and the viscosity of the polymeric electrolytes. EIS of the dual devices at zero bias show the appearance of the charger transfer semicircle, a 100 times increase in the diffusive capacitance and 100 times diminish in the diffusive resistance compared with the single ones. It suggests that for the dual devices, the reduction–oxidation process should initiate at lower applied potentials and the counter-ions could rapidly diffuse into the counter-electrode and largely stored there in comparison with the single ECDs. These results are congruent with the optical kinetics of both types of ECDs, namely, the use of the secondary electroactive coating (PANI) permits a low color switch

potential as well as a high color switch speed in the dual P3MT-based ECDs.

**Acknowledgments** The authors thank José Campos for electrical characterization and Rogelio Morán for technical support. This work was financed by PROMEP (UAEMOR-PTC-66) and CONACyT (42794 and G38618).

## References

1. Akhtar M, Weakliem HA, Paiste RM, Gaughan K (1988) *Synth Met* 26:203
2. Rodrigues MA, De Paolo MA, Mastragostino M (1991) *Electrochim Acta* 36:2143
3. Arbizzani C, Mastragostino M, Zanelli A (1995) *Sol Energy Mater Sol Cells* 39:213
4. Arbizzani C, Mastragostino M, Meneghello L, Morselli M, Zanelli A (1996) *J Appl Electrochem* 26:121
5. Hu H, Hechavarría L, Campos J (2003) *Solid State Ionics* 161:165
6. Hu H, Ortiz BE, Hechavarría L (2007) *Opt Mater* 29:579
7. Nicho ME, Hu H, López Mata C, Escalante J (2004) *Sol Energy Mater Sol Cells* 82:105
8. Corradini A, Marinangeli AM, Mastragostino M (1990) *Electrochim Acta* 35:1757
9. Gazotti WAJr, Casalbore-Miceli G, Geri A, De Paoli MA (1998) *Adv Mater* 10:60
10. Gazotti WAJr, De Paoli MA, Casalbore-Miceli G, Geri A, Zotti G (1999) *J Appl Chem* 29:753
11. Lin TH, Ho HC (2006) *Sol Energy Mater Sol Cells* 90:506
12. Hechavarría L, Hu H, Rincón ME (2003) *Thin Solid Films* 441:56
13. Zweibel K (1984) *Basic Photovoltaic principles and methods*. Reinhold, New York, NY, USA, p 2
14. Macdonald JR (1987) *Impedance spectroscopy: emphasizing solid materials and systems*. Wiley, New York
15. Bruce PG (1987) *Polymer electrolyte reviews* 1. In: MacCallum JR, Vincent CA (eds) Elsevier, London, pp 237–274
16. Armstrong RD, Todd M (1995) *Interfacial electrochemistry*. In: *Solid state electrochemistry*. Burce PG (ed) Cambridge University Press, Cambridge, pp 264–291
17. Leon U, Nicho ME, Hu H, Cruz R (2007) *Sol Energy Mater Sol Cells* (in press)
18. Jütter K, Schmitz RHJ, Hudson A (1999) *Electrochim Acta* 44:4177
19. Tolstoplyatova EG, Sazonova SN, Malev VV, Kondratiev VV (2005) *Electrochim Acta* 50:1565
20. Valaski R, Bozza AF, Micaroni L, Hümmelgen LA (2000) *J Solid State Electrochem* 4:390